ACS OMEGA

http://pubs.acs.org/journal/acsodf

Article

Insights into a Low-Rank Naomaohu Coal Structural Information by Multistage Fractions Coupled with LIAD-VUVPI-TOFMS

Jingxiong Yu, Fanggang Liu, Zefeng Deng, Zaifa Shi, Jiangle Zhang, Qiaolin Wang, Jing Yang, Haoquan Hu, Zhengbo Qin,* and Zichao Tang*

Cite This: *ACS Omega* 2022, 7, 6935−6943

Read Online

ACCESS | Metrics & More | Article Recommendations | Supporting Information

ABSTRACT: In-depth insights into the chemical composition and structural information of coal are an effective way to improve the efficiency of coal utilization. Laser-induced acoustic desorption coupling with vacuum ultraviolet photoionization time-of-flight mass spectrometry (LIAD-VUVPI-TOFMS) was applied to structural characterization of cyclohexane extracts of low-rank Naomaohu coal. The characterization of four types (12 model compounds) of mixed coal model compounds (three compounds per category)—saturated hydrocarbons, substitute aromatic hydrocarbons, aromatic hydrocarbons, and aromatic heteroatom rings—demonstrated that the approach can provide intact molecular weight information. The cyclohexanone extract (E_{CYC}) was obtained by microwave-assisted extraction and separated into four group components (F1−4) by column chromatography to achieve component classification and simplify analysis. The molecular weight and structure were obtained by LIAD-VUVPI-TOFMS and synchronous fluorescence spectroscopy, combined with microwave-assisted extraction and column chromatography to separate product characteristics. Chemical components of a total of 248 species were observed, of which 46 are derived from aliphatic hydrocarbons embedded in the coal skeleton structure, 132 species are derived from aromatic hydrocarbons embedded in the coal skeleton structure, 61 are derived from possible coal skeleton units (compounds have obvious stacking and bonding effects), and 9 could not be determined (aromatic hydrocarbons or a possible coal skeleton structure unit).

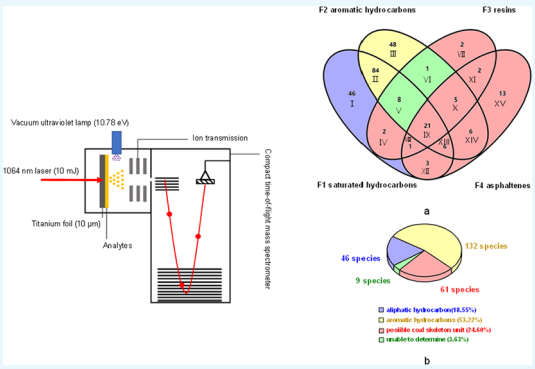

INTRODUCTION

Fossil fuels, mainly coal and oil, still dominate global energy consumption. Fossil fuels will continue to power the world economy for the next few decades.[1,2] Understanding the molecular structure and chemical composition of coal is a key and difficult aspect of coal chemistry.[3] In the process of coal processing and utilization, the reactivity of pyrolysis, liquefaction, and gasification are closely related to the structure of coal.[4] In-depth insights into the structure of coal at the molecular level not only is of important theoretical significance but can also better guide the processing and utilization.[2,5] For example, Shu and Zhang developed an efficient directional direct coal liquefaction technology based on the maceral characteristics of Shenhua coal, which can effectively improve oil yield and lower gas yield.[6] The macromolecular structure of coal is formed by the "polymerization" of many basic structural units with similar but not identical structures. Some structural units are in the extractable phase and some are cross-linked and entangled, forming a three-dimensional structure.[7] Low molecular weight compounds are uniformly dispersed and embedded in the structure and affect the properties. Solvent extraction is an effective method to obtain low-weight molecules from coal.[8,9] During solvent extraction, organic solvents can destroy interaction forces such as hydrogen bonds and van der Waals forces and obtain organic components embedded in the macromolecular network structure.[10] Among many solvent extraction methods (the extraction temperature is higher than 300 °C), microwave-assisted extraction (MAE) can extract efficiently organic components in coal at low temperatures (below 200 °C).[11−13] Mahat et al.[13] found that the extraction rate of MAE for 20 min is 30−40% higher than that of Soxhlet extraction for 72 h. A higher extraction rate also provides greater structural information.

The physical and chemical properties of coal can be obtained by a variety of characterization methods, such as HRTEM, Raman spectroscopy, NMR, and so forth.[10,14] However, these characterization methods can provide only general information on the types of chemical classes or the presence of certain functional groups. To obtain abundant

Received: November 23, 2021
Accepted: February 8, 2022
Published: February 17, 2022

https://doi.org/10.1021/acsomega.1c06619
ACS Omega 2022, 7, 6935−6943

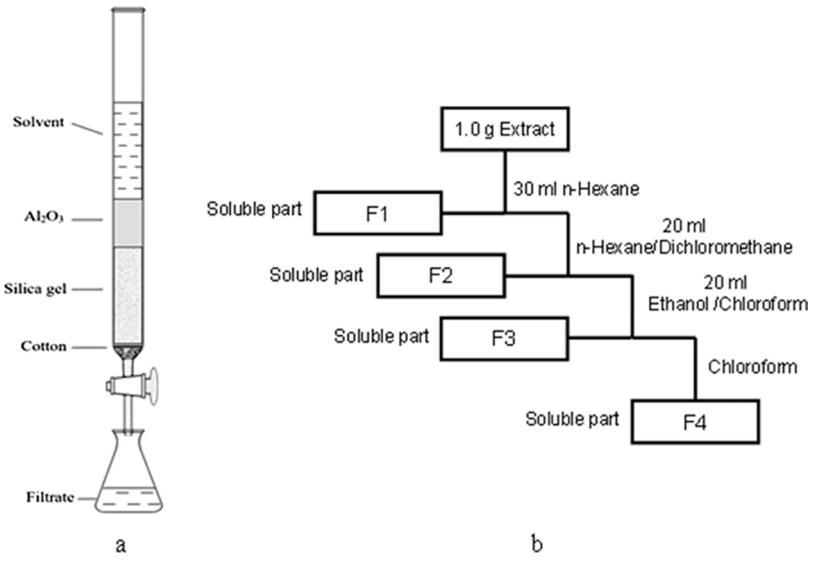

Figure 1. (a) Apparatus of column chromatography. (b) Procedure for column chromatography of extract.

information on coal structure, mass spectrometry data are desirable. For complex solid samples, thermal desorption is a conventional desorption method, but heat treatment destroys the structural integrity of analytes.[15] The acquisition of detailed molecular information on coal has always been a key and difficult aspect in coal chemistry research.[16,17] Laser-induced acoustic desorption (LIAD) is a gentle mass spectrometry desorption technique that ensures the integrity of analytes. LIAD uses acoustic waves and shockwaves generated by laser bombardment of a metal foil to transfer an appropriate amount of energy to the analytes located on the opposite side of the irradiated foil for gentle desorption. Both non-volatiles and thermally labile analytes achieve efficient and intact desorption.[18−20] Different from matrix-assisted laser desorption/ionization (MALDI)[21] and electrospray ionization (ESI),[22] LIAD possesses unique features as it desorbs intact neutral molecules instead of direct formation of ions. In theory, LIAD can be combined with electron ionization (EI), photoionization (PI), chemical ionization (CI), and other ionization methods to analyze all desorbable analytes without being restricted by their polarity.[23] By combining LIAD with different types of mass spectrometers and ionization sources, the molecular weight characterization of saturated hydrocarbons, petroleum aromatic hydrocarbons, and peptides from a heavy oil was realized.[20,24,25]

However, this technique has not yet been applied to coal. TOFMS coupling with LIAD and VUVPI[26] techniques can obtain intact mass spectral information on organic molecules. In this work, four types of coal model compounds—saturated hydrocarbons, substituted aromatic hydrocarbons, aromatic hydrocarbons, and heteroatom ring aromatic compounds—are used to evaluate the feasibility and mass spectrum characteristics of LIAD-VUVPI-TOFMS in coal structure research. Low-rank Naomaohu (NMH) coal (Xinjiang, China) is extracted by MAE using cyclohexanone (CYC), and the extract (E_{CYC}) is further separated by column chromatography to obtain the four components: saturated hydrocarbons (F1), aromatic hydrocarbons (F2), resins (F3), and asphaltenes (F4). The mass spectra of E_{CYC} and fractionate F1−4 characterized by LIAD-VUVPI-TOFMS are used to reflect the low-weight molecule distribution and structural characteristics of this coal.

EXPERIMENTAL SECTION

Materials. Twelve selected coal model compounds with >99% purity, listed in Table S1, were purchased from Aladdin Chemistry Co., Ltd., China. Low-rank NMH coal purchased from Xinjiang province was crushed to sizes below 100 μm and dried in a vacuum oven at 60 °C for 24 h. The results of proximate and ultimate analyses of coal samples are listed in Table S2.

Microwave-Assisted Extraction. MAE was conducted on a microwave extraction apparatus (MAS-II, Sineo Microwave Science and Technology, Ltd.), equipped with a water-cooled reflux condenser. About 5 g of coal and 100 mL of cyclohexane were added in a glass flask, and then, MAE was performed at 125 °C for 1 h. Then, the extract (E_{CYC}) was dried in a vacuum oven at 80 °C.

Group Component Separation. The separation of group components was done as per the analysis method for fractions of rock extract and crude oil (Petroleum and Natural Gas Industry Standard of the People's Republic of China, SY/T 5119-2008).[27] The extract was divided into 4 group components by column chromatography; the apparatus and procedure of separation are shown in Figure 1a,b. First, the absorbent cotton was eluted with chloroform until there was no fluorescence. The chromatography silica gel was activated at 130 °C for 8 h and neutral alumina at 425 °C for 4 h. The appropriate amount of absorbent cotton, 3 g of chromatography silica gel, and 2 g of neutral alumina were added to a glass chromatographic column in that order.

The synchronous fluorescence (SF) spectroscopy analysis of E_{CYC} and its group components was conducted on a Hitachi F-7000 spectrophotometer at 1200 nm/min scan rate and 2.5 nm slit width. The difference in value between excitation and emission wavelength was fixed as 14 nm. The solutions were diluted by dichloromethane before analysis. To avoid the self-absorption effect, a scan range of 200−800 nm was selected. The details are similar to those of previous work.[28]

LIAD-VUVPI-TOFMS Experiments. All experiments were performed on a compact TOFMS[29] equipped with a LIAD

https://doi.org/10.1021/acsomega.1c06619
ACS Omega 2022, 7, 6935−6943

desorption source and a VUVPI ionization source (LIAD-VUVPI-TOFMS), shown in Figure 2. In each experiment,

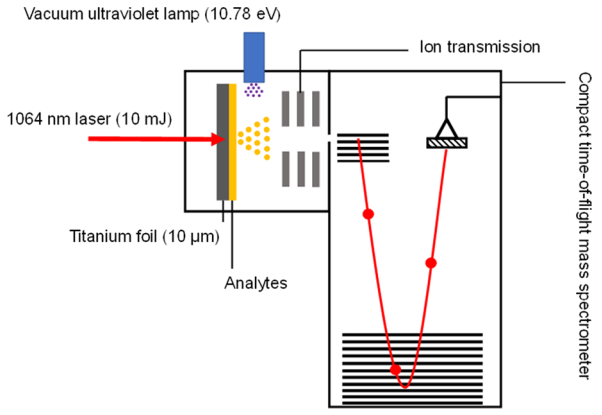

Figure 2. Scheme diagram of LIAD-VUVPI-TOFMS.

analytes were deposited on a titanium foil (thickness 10 μm, radius 10 mm), and the opposite side of the titanium foil was supported by a quartz plate and irradiated by a pulsed laser (wavelength: 1064 nm, pulse energy: 10 mJ, pulse width: 7−10 ns, frequency: 10 Hz). The titanium foil could be rotated 360°, and approximately 5% of the foil's total surface area could be irradiated by laser. After laser irradiation, the analytes entered the gas phase and were "soft" ionized by VUV light, which was provided by a VUV lamp (Hamamatsu, L13301, 10.78 eV, and 8.5 W), and the vacuum in the ionization area was maintained at ~7 × 10^{-4} Pa to ensure ionization efficiency. Molecular weight information was finally detected by TOFMS (R > 1500). More detailed parameters of the compact TOFMS have been described in past works.[9,29,30] The LIAD-VUVPI-TOFMS mentioned in this work is a self-developed substrate-enhanced LIAD MS, which is over 5 times more sensitive than traditional LIAD MS, and its detailed performance parameters and testing procedures have been reported in detail.[31]

Sample preparation: For the mixed model compounds, 10 mg of three model components of the same type were dissolved in 1 mL of solvent (ethanol or acetone). For the 12 model compounds, E_{CYC}, and F1−4, 10 mg analytes were dissolved in 1 mL of solvent, which was the corresponding extraction solvent and elution solvent. Then, 20 μL of the prepared solution was deposited on the titanium foil, which was dried at 40 °C.

RESULTS AND DISCUSSION

LIAD-VUVPI-TOFMS Characterization of Coal Model Compounds. The composition and structure of coal are too complex to be studied directly. Therefore, coal model compounds are widely used in the research of coal chemistry because of their ability to reflect the properties of coal to a certain extent. Four kinds of representative coal model compounds were used to verify the feasibility of LIAD-VUVPI-TOFMS in coal composition analysis. Each kind of mixed model compounds includes three compounds with the same concentration. The photoionization mass spectra shown in Figure 3 were used to evaluate the LIAD-VUVPI-TOFMS characteristics of the complex.

Consistent with expectations, a mass spectrum with fragment-free peaks can be obtained by the combination of

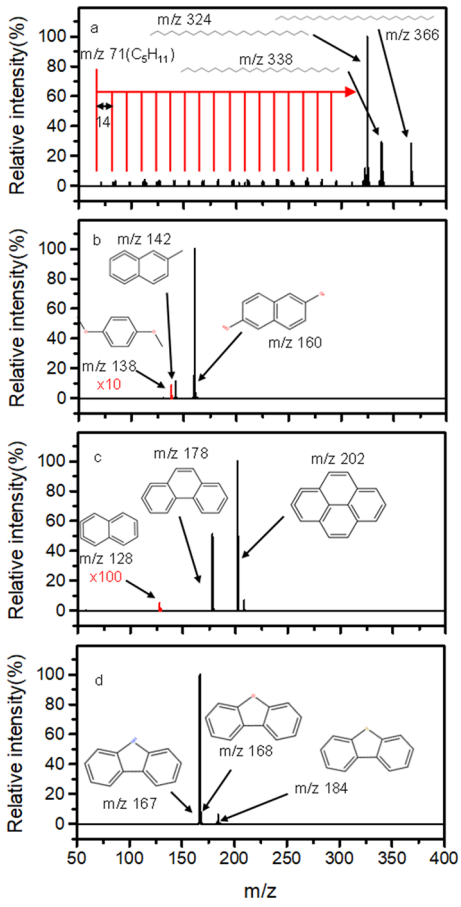

Figure 3. LIAD-VUVPI-TOFMS mass spectra of saturated hydrocarbons: (a) *n*-tricosane, *n*-tetracosane, and *n*-nexacosane; substitute aromatic hydrocarbons: (b) 1,4-dimethoxybenzene, 2-methylnaphthalene, and 2,6-naphthalenediol; aromatic hydrocarbons: (c) naphthalene, phenanthrene, and pyrene]; and aromatic heteroatom rings: (d) dibenzothiophene, dibenzofuran, and carbazole.

soft desorption LIAD and soft ionization VUVPI (LIAD-VUVPI-TOFMS). As is seen in Figure 3b−d, the mass spectra of substitute aromatic hydrocarbons (1,4-dimethoxybenzene, 2-methylnaphthalene, and 2,6-naphthalenediol) (Figure 3b), aromatic hydrocarbons (naphthalene, phenanthrene, and pyrene) (Figure 3c), and aromatic heteroatom rings (dibenzothiophene, dibenzofuran, and carbazole) (Figure 3d) are all molecular ion peaks with fragment-free peaks. Different from this, Figure 3a shows that there were a series of fragment peaks with a molecular weight difference of 14 (CH_2), except the obvious molecular ion peaks, in the mass spectrum of saturated hydrocarbons (*n*-tricosane, *n*-tetracosane, and *n*-nexacosane). However, there is no fragmentation peak in the saturated hydrocarbon mass spectrum obtained by chemical ionization combined with LIAD by Campbell et al.[23c] The fragment generation should come from the photoionization process in this work. When the energy of VUV light far exceeds the ionization threshold of saturated hydrocarbon, the saturated hydrocarbons produce photofragments.[32] In Figure 3a, the smallest fragment peak is m/z = 71, which is ascribed to the C_5H_{11} fragment from the H abstraction of pentane (C_5H_{12}). The ionization energy of saturated hydrocarbons with different carbon numbers (Figure S1) revealed that the ionization energy of saturated hydrocarbons decreases as the number of carbon increases. The ionization energy of methane,

https://doi.org/10.1021/acsomega.1c06619
ACS Omega 2022, 7, 6935−6943

ethane, and propane is higher than that of the VUV lamp (10.78 eV) and cannot be ionized. Starting from butane (10.58 eV), the ionization energies of saturated hydrocarbons are all lower than the ionization energy of the VUV lamp, and the ionization energy of butane (10.58 eV) and pentane (10.28 eV) are closer to 10.78 eV to achieve complete ionization. For hexane (10.13 eV) and higher carbon number alkanes, the ionization energy is at least 0.65 eV lower than the energy of the VUV lamp, which is prone to breakage of C−C bonds. Despite the presence of fragment peaks, the peak intensity of saturated hydrocarbon molecular ion peaks is still much higher than that of fragment peaks. In addition, the stable interval and intensity rules of the fragment peaks make it easy to judge. At the same time, the characteristic peak at m/z = 71 is an important evidence for judging the existence of long linear saturated hydrocarbons. Furthermore, eight coal model compounds and a random combination of four coal model compounds were characterized, and their LIAD-VUVPI-TOFMS spectra are shown in Figures S2 and S3. The eight coal model compounds are carbazole, dibenzothiophene, 2-methylnaphthalene, 1,4-dimethoxybenzene, phenanthrene, pyrene, *n*-tricosane, and *n*-nexacosane.

Unfortunately, the intensity information in LIAD-VUVPI-TOFMS does not accurately reflect the quantitative characteristics of the analytes. As seen in Figure 3c, the peak intensity of pyrene is about 2000 times than that of naphthalene with the same concentration. It is worth noting that the absolute photoionization cross sections of naphthalene, phenanthene, and pyrene are roughly the same at 9.8 eV.[33] The LIAD process is the main cause of relative intensity gap. Similar phenomena also occur in other types of mixtures (Figure 3a−d). The mechanism of LIAD is currently unclear, and a uniform law cannot be derived from parameters such as ionization energy, boiling point, and molecular weight.[18] However, LIAD-VUVPI-TOFMS is feasible in the composition analysis of complex organics. For LIAD-VUVPI-TOFMS, the peak intensity of the mass spectrum can provide only a limited reference for the content of each analyte.

LIAD-VUVPI-TOFMS and SF Analysis of E_{CYC} and Its Group Components. The composition and structure of coal are very complex, and it is not realistic to analyze coal directly. Low molecular weight extracts are important media for analyzing coal's structural characteristics. Using the MAE method with CYC as the solvent, the extract yield can reach 8.0 wt % (the formula of the extraction rate is given in the Supporting Information), which is higher than that of other solvents, and 1 h for NMH coal.[28] E_{CYC} accounts for about 8.7 wt % of coal organic matter. The mass spectrum of LIAD-VUVPI-TOFMS of E_{CYC} is shown in Figure 4. It is generally

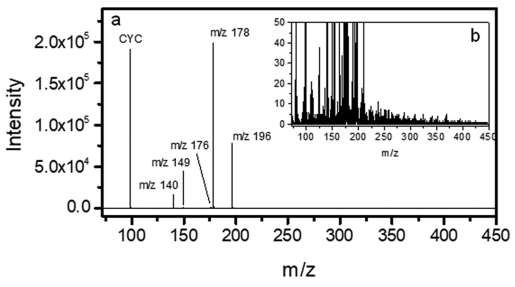

Figure 4. LIAD-VUVPI-TOFMS mass spectrum of E_{CYC}: (a) high-intensity peak signal and (b) low-intensity peak signal.

believed that a mass spectral peak, whose signal-to-noise ratio is greater than or equal to 3, is considered a valid signal. The average noise in E_{CYC}'s mass spectrum is less than 1. This means that all signals, with intensity greater than or equal to 3, are valid mass spectral peaks. Even if the extract can reflect only the molecular structure information of the coal part, it still contains more than 179 compounds (existence of isomers), distributed in the range m/z 70−396. At the same time, the peak intensities of species at m/z = 140, 149, 176, 178, and 196 are much higher than those of other compounds. Just as the discussion in the previous section, the peak intensity is affected by both desorption efficiency and photoionization efficiency. Other species with low signal intensity may also occupy a non-negligible content in E_{CYC}.

Laser desorption/ionization (LDI) MS and MALDI MS are common methods used by researchers to characterize coal composition information.[17,34] As a high-energy desorption/ionization method, LDI MS inevitably generates a large number of fragment ions, which can only roughly determine the mass distribution range for complex analytes, but certainly not precisely. MALDI is widely used in the detection of organic molecules as a gentle mass spectrometry detection technique. Figure 5 shows the mass spectra of E_{CYC} by MALDI MS using different matrices {sinapinic acid (SA), *trans*-2-[3-(4-*tert*-butylphenyl)-2-methyl-2-propenylidene]malononitrile (DCTB), 2,5-dihydroxybenzoic acid (DHB), and α-cyano-4-hydroxycinnamic acid (CHCA)}. Unfortunately, the mass range of the matrix required by MADLI MS is distributed in the range m/z 0−500 (SA m/z 224, DCTB m/z 250, DHB m/z 154, and CHCA m/z 189), and the fragments and clusters produced by the matrix under the action of the laser interfere with the final analysis. The high baseline produced by the matrix can be clearly seen in Figure 5b,c. In addition, the spectral information obtained by different matrices is not completely the same due to the selectivity of the matrix to the ionized object (Figure 5). At the same time, the E_{CYC} species abundance obtained by MALDI MS is far less than that obtained by LIAD-VUVPI-TOFMS. For E_{CYC}, LIAD-VUVPI-TOFMS is obviously a more suitable analysis method.

Aliphatic hydrocarbon compounds do not produce fluorescence after absorbing photons, but SF spectrum can determine the distribution of aromatic rings in complex systems,[35] combining the SF spectrum of standard aromatic substances and the "red shift" of fluorescence peaks caused by alkyl and heteroatom substituents.[36] The relationship between the number of aromatic rings and the fluorescence wavelength is as follows: monocyclic aromatic hydrocarbons (300−375 nm), bicyclic aromatic hydrocarbons (375−425 nm), tricyclic aromatic hydrocarbons (425−475 nm), and tetracyclic aromatic hydrocarbons and aromatics above four rings (>475 nm). Assignment of SF compound spectral peaks of conventional aromatics was done as per the reports of Wang et al.[37] In the SF spectrum, monocyclic aromatic hydrocarbons mainly include benzene and biphenyl structures, bicyclic aromatic hydrocarbons mainly include naphthalene structures, tricyclic aromatic hydrocarbons mainly include anthracene or phenanthrene structures, and tetracyclic aromatic hydrocarbons and aromatics above four rings are mainly fused rings with four or more rings. The SF spectrum of E_{CYC} were peak fitted as shown in Figure 6a. The characteristic peaks attributed to monocyclic aromatic hydrocarbons and bicyclic aromatic hydrocarbons have the highest intensity, followed by tricyclic aromatic hydrocarbons. The aromatic compounds in E_{CYC} are

https://doi.org/10.1021/acsomega.1c06619
ACS Omega 2022, 7, 6935−6943

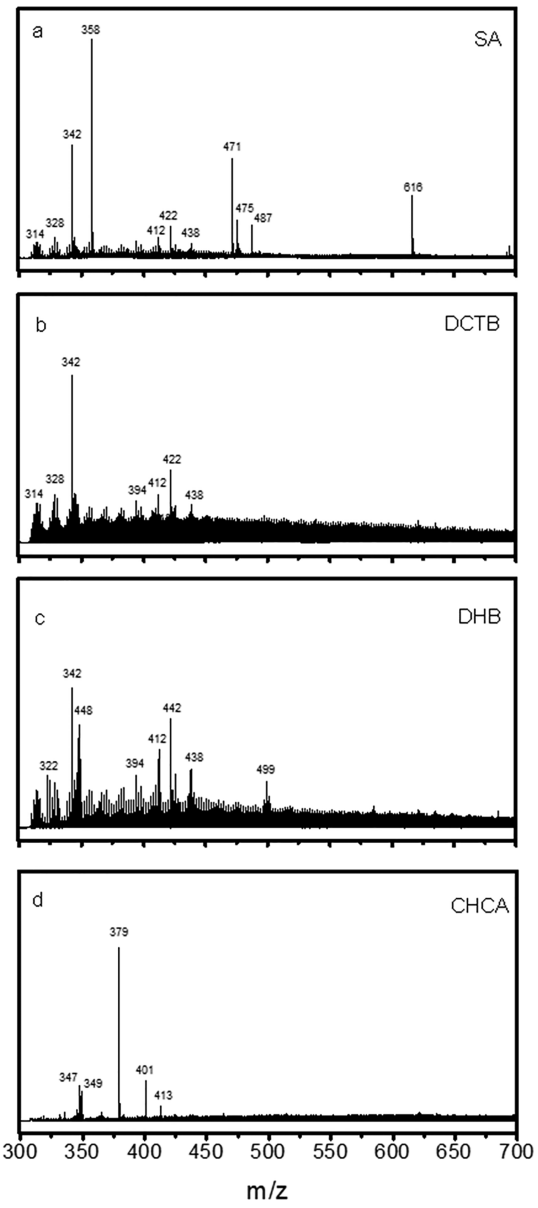

Figure 5. MALDI MS mass spectrum of E_{CYC}: (a) SA, (b) DCTB, (c) DHB, and (d) CHCA.

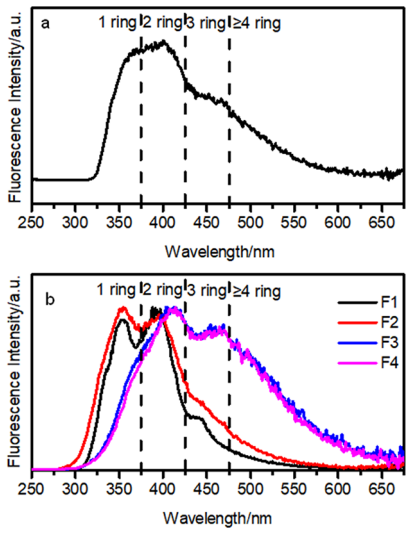

Figure 6. SF spectra of (a) E_{CYC} and (b) group components F1, F2, F3, and F4.

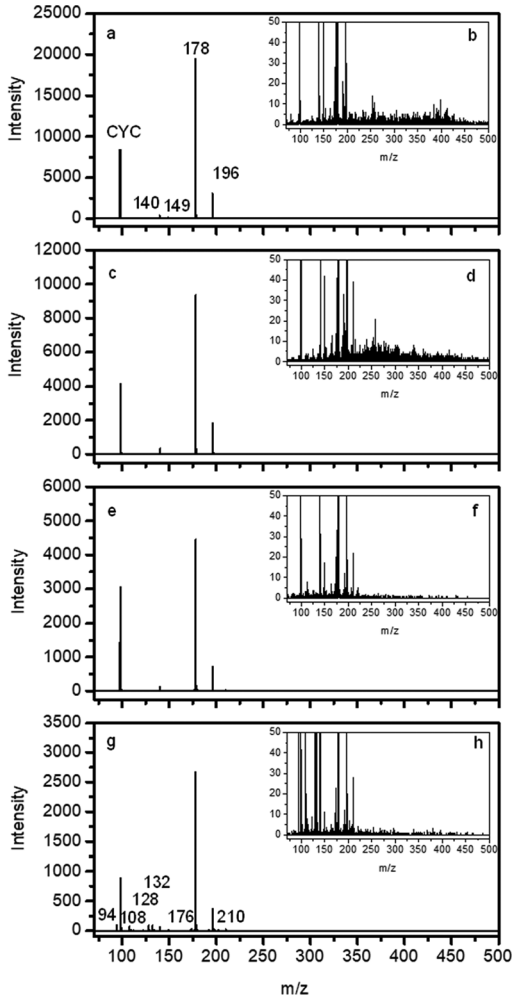

Figure 7. LIAD-VUVPI-TOFMS mass spectra of group components F1 (a,b), F2 (c,d), F3 (e,f), and F4 (g,h) [(b,d,f,h) are also shown in Figure S4].

mainly 1−3 rings, including a small number of structures containing four or more aromatic rings.

Column chromatography is a commonly used method for the pretreatment of complicated samples and widely used in the separation of petroleum components and coal-derived liquids.[11,38] Although the structural complexity and molecular weight distribution of the extract are simplified, it is still a complex mixture. The E_{CYC} is further fractionated by column chromatography separation method SY/T5119-2008.[27] E_{CYC} can be fractionated into four group components: saturated hydrocarbons (F1), aromatic hydrocarbons (F2), resins (F3), and asphaltenes (F4). The four components are all characterized by LIAD-VUVPI-TOFMS. The mass spectrum of F1−4 (Figure 7) showed obvious peak crossing, especially the molecular weights of m/z 140, 149, 176, 178, and 196, which exhibit the strongest signal among the four group components. This is because the SY/T5119-2008 column separation method is mainly designed for crude oil and heavy oil. Component crossover is a common problem in column chromatography, such as monocyclic aromatic hydrocarbons entering saturated hydrocarbon components.[39] Meanwhile, F4

https://doi.org/10.1021/acsomega.1c06619
ACS Omega 2022, 7, 6935−6943

and F3 fractions have a lower average molecular weight distribution compared to F1 and F2. Resins (F3) and asphaltenes (F4) are mainly aromatic hydrocarbons with condensed ring structures.[25,40] Besides, the continuous decrease in the intensity of the F1-to-F4 mass spectrum potentially from some compounds in E_{CYC} can cross-link and stack to hinder LIAD desorption. This phenomenon indicates that CYC not only extracts the low molecular weight organic matter in the coal but also overcomes the hydrogen bonds in the coal skeleton structure, van der Waals forces, and other weak interaction forces.

All mass peaks in the mass spectra of the four fractions (F1−4) are classified by the four-dimensional Venn diagram shown in Figure 8a.[41] Detailed molecular mass weight information is given in Table S1. Because the VUV lamp has a fixed luminous flux, the sensitivity of LIAD-VUVPI-TOFMS for low-content compounds can be effectively improved by simplifying the composition of complex analytes. A total of 248 different mass peaks are obtained from the four fractions (F1−4), occupying the mass range of m/z 94−464. The combination of column chromatography and LIAD-VUVPI-TOFMS significant increases the abundance of mass spectrum information. However, it is extremely difficult to achieve complete separation of family components through column chromatography. Incomplete separation and possibly cross-contamination are revealed by HPLC re-chromatography of fractions derived from column chromatography separation methods by Bissada et al.[39] Bissada et al. also summarized the cross-contamination characteristics between fractions.[39] Their asphaltene fraction has only resin pollution, but it exists in 4 fractions at the same time; ideal aromatic compounds are present only in saturated hydrocarbons and aromatic hydrocarbon fractions; and saturated hydrocarbons are mainly present in saturated hydrocarbons and resin fractions. The component overlap rule of fractions separated by column chromatography is combined with the molecular weight information and SF spectrum information of each fraction (Figure 5b) to preliminarily derive the composition and structure of E_{CYC}. First, the unique characteristic mass peaks of each fraction are classified as their corresponding fractions: F1 (saturated hydrocarbons, Figure 8a-I) 46 species, F2 (aromatic hydrocarbons, Figure 8a-III) 48 species, F3 (resins, Figure 8a-VII) 2 species, and F4 (asphaltenes, Figure 8a-iii) 13 species. Next, because the asphaltene fraction contains only resins except asphaltene, the species in Figure 8a-VIII−XIV belong to resins and asphaltene. At the same time, the resin fraction does not contain saturated hydrocarbon; the species in Figure 8a-IV belong to resins, and the species in Figure 8a-IV belong to resins or aromatic hydrocarbons. F1 as a saturated hydrocarbon fraction should not have fluorescence effect in principle, but it shows a high similar SF spectrum with F2. The high similarity of SF spectrum between F1 and F2 can be attributed to the compounds that exist only in F1 and F2 (Figure 8a-XIV), with component overlap rule of aromatic hydrocarbon components and saturated hydrocarbon components; most of the species in Figure 8a-II should be aromatic hydrocarbons. For the 9 species belonging to Figure 8a-V,VI, due to the serious cross-contamination of aromatic hydrocarbons and colloidal fractions, it can only be determined that they are resins or aromatic hydrocarbon species. In conclusion (Figure 8b), it can be determined that E_{CYC} contains 46 species of saturated hydrocarbons (Figure 8a-I), 132 species of aromatic hydrocarbons (Figure 8a-II,III), 61 species of resins and asphaltenes (Figure 8a-IV−XV), and 9 species that could not be determined species (aromatic hydrocarbons or resins) (Figure 8a-V,VI).

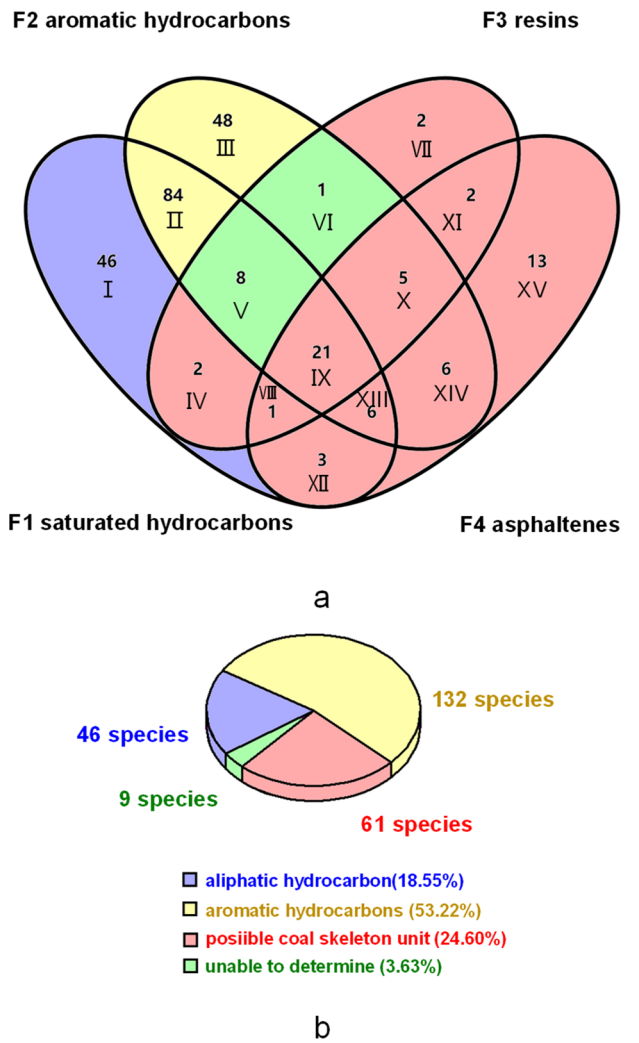

Figure 8. (a) Four-dimensional venn diagram of mass spectrum distribution of group components saturated hydrocarbons (F1), aromatic hydrocarbons (F2), resins (F3), asphaltenes (F4). (b) distribution of aliphatic hydrocarbons, aromatic hydrocarbons, and possible coal skeleton unit compounds in E_{CYC}.

Based on the spectral information of SF, the aromatic ring structure information of aromatic hydrocarbons, resins, and asphaltenes is further deduced. According to the SF spectrum information of F2 fraction, F2 should be mainly 1-ring or 2-ring aromatics and a small number of ≥3-ring aromatic hydrocarbons. The SF spectra of the F3 and F4 fractions are highly coincident, and they have a significant fluorescence response in the ≥2-ring regions, while the fluorescence signal in the 1-ring region is significantly lower than that of the F2 fraction. Compared with F1 and F2, the SF spectra of F3 and F4 have obvious fluorescence response in the region with ≥3 rings; the F3 and F4 fractions contain most of the polycyclic aromatic hydrocarbons in E_{CYC}. In view of cross-contamination law of the fractions, a small number of ≥3-ring aromatic hydrocarbons in the F2 fraction should come from the F3 fraction. The aromatic hydrocarbons in E_{CYC} should mainly contain aromatic structure of 1−2 rings such as benzene,

https://doi.org/10.1021/acsomega.1c06619
ACS Omega 2022, 7, 6935−6943

biphenyl, and naphthalene structures. At the same time, the fluorescence peak position of the SF spectra of F2 in the 2-ring region is significantly blue-shifted compared to the fluorescence peak of the SF fluorescence spectra of F3 and F4 in the 2-ring region, which shows that F2 and F3 and F4 have different fluorescent species in the 2-ring regions. F3 and F4 are divided into resins and asphaltenes in the analysis of petroleum components. However, the MAE process mainly extracts organic molecules embedded in the coal skeleton structure and coal skeleton structural units obtained by destroying weak interaction forces. In the separation process of E_{CYC} by column chromatography, the aliphatic and aromatic hydrocarbons embedded in the coal skeleton structure should be separated first, and the rest can be retained by accumulation and bonding effect similar to resins and asphaltenes. Stacking and bonding effects are important forms of coal skeleton formation. The first eluted saturated hydrocarbons (46 species) and aromatic hydrocarbons (132 species) are attributed to the small molecules embedded in the coal skeleton structure due to their lack of obvious stacking and bonding effects (Figure 7b). Based on the obvious bonding and stacking effects in F3 and F4 (61 species), it may come from the coal skeleton structural unit obtained by breaking the weak interaction between molecules (Figure 8b). Although the coal skeleton structural unit species in E_{CYC} account for only 24.6% of the species, MS peak intensity information shows that its content in E_{CYC} has an overwhelming advantage. Almost all the characteristic species with a high mass spectrum peak intensity are classified into possible coal skeleton structural units. The most obvious mass (m/z 178) is that of phenanthrene or anthracene, which is consistent with the results obtained by Xiong et al.[42] through hydrogen peroxide oxidation degradation of NMH coal. At the same time, the coal skeleton structural unit contains not only polycyclic aromatic hydrocarbons but also aromatic compounds with 1−4 rings (Figure 8b), which is characterized by the ability to form stacking and bonding effects through weak intermolecular interactions. In conclusion, the species of E_{CYC} can be classified as aliphatic hydrocarbons (46 species) embedded in the coal skeleton structure; aromatic hydrocarbons (132 species) mainly with 1-ring or 2-ring aromatic structures embedded in the coal skeleton structure; a possible coal skeleton structure unit (61 species) containing 1−4-ring aromatic ring structure at the same time; and species that could not be determined (9 species, aromatic hydrocarbons or a possible coal skeleton structure unit).

CONCLUSIONS

In this work, LIAD-VUVPI-TOFMS is proved to be a novel method for characterizing coal molecular information. Except for saturated hydrocarbons, which produce a small number of fragment peaks, most of the compounds in coal can be detected without fragmentation. Using NMH coal as a model, LIAD-VUVPI-TOFMS is applied to the study of complex real samples. On the basis of MAE, E_{CYC} is simplified to F1 (aliphatic hydrocarbon), F2 (aromatic hydrocarbon), F3 (resins), and F4 (asphaltenes) through column chromatography, further simplifying the analysis. Through LIAD-VUVPI-TOFMS, it can be determined that E_{CYC} contains at least 248 compounds. Combined with the SF spectroscopy and component overlap rule of fractions, 96.4% species in E_{CYC} are classified accurately. The compounds in E_{CYC} are divided into aliphatic hydrocarbons embedded in the coal skeleton structure (46 species), aromatic hydrocarbons embedded in the coal skeleton structure (132 species), possible coal skeleton structural unit compounds (61 species), species that could not be determined (9 species, aromatic hydrocarbons or a possible coal skeleton unit). Monocyclic aromatic hydrocarbons and bicyclic aromatic hydrocarbons are the main constructing forms of aromatic hydrocarbons in E_{CYC}, followed by tricyclic aromatic hydrocarbons. The compounds with the highest content in E_{CYC} should come from possible coal skeleton unit compounds, which are mainly polycyclic aromatic hydrocarbons and 1−4-rings aromatic ring structures at the same time. LIAD-VUVPI-TOFMS can provide accurate molecular weight information without being affected by the polarity and thermal instability of analytes. In combination with other characterization methods and sample pretreatment methods, MAE in this work is an innovative idea and method for the study of coal chemical structure, which can provide data support for the efficient utilization of coal at the molecular level.

ASSOCIATED CONTENT

Supporting Information

The Supporting Information is available free of charge at https://pubs.acs.org/doi/10.1021/acsomega.1c06619.

Definition and calculation method of extraction rate, ionization energy of *n*-alkanes, LIAD-VUVPI-TOFMS mass spectra of eight coal model compounds, LIAD-VUVPI-TOFMS mass spectra of the random combination from coal model compounds, LIAD-VUVPI-TOFMS mass spectra of group components, model compound parameter information, proximate and ultimate analyses of NMH coal sample, and cross summary of fractions (PDF)

AUTHOR INFORMATION

Corresponding Authors

Zhengbo Qin − *Anhui Province Key Laboratory of Optoelectric Materials Science and Technology, School of Physics and Electronic Information, Anhui Normal University, Wuhu 241002, China;* orcid.org/0000-0002-1127-8070; Email: wave0403@163.com

Zichao Tang − *State Key Laboratory of Physical Chemistry of Solid Surfaces, College of Chemistry and Chemical Engineering, Xiamen University, Xiamen, Fujian 361005, China*; Email: zctang@xmu.edu.cn

Authors

Jingxiong Yu − *State Key Laboratory of Physical Chemistry of Solid Surfaces, College of Chemistry and Chemical Engineering, Xiamen University, Xiamen, Fujian 361005, China*

Fanggang Liu − *State Key Laboratory of Physical Chemistry of Solid Surfaces, College of Chemistry and Chemical Engineering, Xiamen University, Xiamen, Fujian 361005, China; State Key Laboratory of Fine Chemicals, Institute of Coal Chemical Engineering, School of Chemical Engineering, Dalian University of Technology, Dalian 116024, China*

Zefeng Deng − *State Key Laboratory of Physical Chemistry of Solid Surfaces, College of Chemistry and Chemical Engineering, Xiamen University, Xiamen, Fujian 361005, China*

https://doi.org/10.1021/acsomega.1c06619
ACS Omega 2022, 7, 6935−6943

Zaifa Shi − *State Key Laboratory of Physical Chemistry of Solid Surfaces, College of Chemistry and Chemical Engineering, Xiamen University, Xiamen, Fujian 361005, China*

Jiangle Zhang − *State Key Laboratory of Physical Chemistry of Solid Surfaces, College of Chemistry and Chemical Engineering, Xiamen University, Xiamen, Fujian 361005, China*

Qiaolin Wang − *Anhui Province Key Laboratory of Optoelectric Materials Science and Technology, School of Physics and Electronic Information, Anhui Normal University, Wuhu 241002, China; Key Laboratory of High Power Laser and Physics, Chinese Academy of Sciences, Shanghai 201800, China*

Jing Yang − *State Key Laboratory of Physical Chemistry of Solid Surfaces, College of Chemistry and Chemical Engineering, Xiamen University, Xiamen, Fujian 361005, China*

Haoquan Hu − *State Key Laboratory of Fine Chemicals, Institute of Coal Chemical Engineering, School of Chemical Engineering, Dalian University of Technology, Dalian 116024, China;* orcid.org/0000-0002-5288-2186

Complete contact information is available at: https://pubs.acs.org/10.1021/acsomega.1c06619

Author Contributions

J.Y. and F.L. contributed equally. The manuscript was written through contributions of all authors. All authors have given approval to the final version of the manuscript.

Notes

The authors declare no competing financial interest.

■ ACKNOWLEDGMENTS

This research was supported by the National Key Research and Development Program of China (2016YFB0600301), the National Science Foundation of China (21873003 and 91961107), and National Natural Science Foundation of China Youth Science Fund (21805231). This work was also supported by the Institute of Energy, Hefei Comprehensive National Science Center (GXXT-2020-004), and Open Foundation of Key Laboratory of High Power Laser and Physics, Chinese Academy of Sciences (SGKF202106).

■ REFERENCES

(1) Jiang, K.; Feron, P.; Cousins, A.; Zhai, R.; Li, K. Achieving Zero/Negative-Emissions Coal-Fired Power Plants Using Amine-Based Postcombustion CO2 Capture Technology and Biomass Cocombustion. *Environ. Sci. Technol.* **2020**, *54*, 2429−2438.

(2) Rus'ianova, N. D.; Maksimova, N. E.; Jdanov, V. S.; Butakova, V. I. Structure and reactivity of coals. *Fuel* **1990**, *69*, 1448−1453.

(3) Iino, M. Network structure of coals and association behavior of coal-derived materials. *Fuel Process. Technol.* **2000**, *62*, 89−101.

(4) Mochida, I.; Okuma, O.; Yoon, S.-H. Chemicals from Direct Coal Liquefaction. *Chem. Rev.* **2014**, *114*, 1637−1672.

(5) Levine, D. G.; Schlosberg, R. H.; Silbernagel, B. G. Understanding the chemistry and physics of coal structure (A Review). *Proc. Natl. Acad. Sci. U.S.A.* **1982**, *79*, 3365−3370.

(6) Shu, G.; Zhang, Y. Research on the maceral characteristics of Shenhua coal and efficient and directional direct coal liquefaction technology. *Int. J. Coal Sci. Technol.* **2014**, *1*, 46−55.

(7) (a) Given, P. H.; Marzec, A.; Barton, W. A.; Lynch, L. J.; Gerstein, B. C. The concept of a mobile or molecular-phase within the macromolecular network of coals - a debate. *Fuel* **1986**, *65*, 155−163. (b) Derbyshire, F.; Marzec, A.; Schulten, H.-R.; Wilson, M. A.; Davis, A.; Tekely, P.; Delpuech, J.-J.; Jurkiewicz, A.; Bronnimann, C. E.; Wind, R. A.; Maciel, G. E.; Narayan, R.; Bartle, K.; Snape, C. Molecular structure of coals: A debate. *Fuel* **1989**, *68*, 1091−1106.

(8) Zheng, Q.; Morimoto, M.; Sato, H.; Takanohashi, T. Molecular composition of extracts obtained by hydrothermal extraction of brown coal. *Fuel* **2015**, *159*, 751−758.

(9) Yang, Z.; Wei, X.-Y.; Li, Z.-X.; Zhang, M.; Teng, D.-G.; Zong, Z.-M. Comparative studies on the structural features of soluble portions from thermal dissolution/methanolysis and catalytic hydroconversion of an extraction residue from Heishan lignite. *Fuel* **2019**, *241*, 1138−1144.

(10) Zhang, X.; Zhang, S.; Li, P.; Ding, Z.; Hao, Z. Investigation on solubility of multicomponents from semi-anthracite coal and its effect on coal structure by Fourier transform infrared spectroscopy and X-ray diffraction. *Fuel Process. Technol.* **2018**, *174*, 123−131.

(11) Zhang, L.; Hu, S.; Chen, Q.; Xiao, L.; Syed-Hassan, S. S. A.; Jiang, L.; Wang, Y.; Su, S.; Xiang, J. Molecular structure characterization of the tetrahydrofuran-microwave-extracted portions from three Chinese low-rank coals. *Fuel* **2017**, *189*, 178−185.

(12) Ge, L.; Zhang, Y.; Wang, Z.; Zhou, J.; Cen, K. Effects of microwave irradiation treatment on physicochemical characteristics of Chinese low-rank coals. *Energy Convers. Manage.* **2013**, *71*, 84−91.

(13) Mahat, R. K.; Rodgers, W.; Basile, F. Microwave Radiation Heating in Pressurized Vessels for the Rapid Extraction of Coal Samples for Broad Spectrum GC-MS Analysis. *Energy Fuels* **2014**, *28*, 6326−6335.

(14) (a) Díaz, C.; Blanco, C. G. NMR: A powerful tool in the characterization of coal tar pitch. *Energy Fuels* **2003**, *17*, 907−913. (b) Jubb, A. M.; Botterell, P. J.; Birdwell, J. E.; Burruss, R. C.; Hackley, P. C.; Valentine, B. J.; Hatcherian, J. J.; Wilson, S. A. High microscale variability in Raman thermal maturity estimates from shale organic matter. *Int. J. Coal Geol.* **2018**, *199*, 1−9.

(15) Tobias, H. J.; Ziemann, P. J. Compound identification in organic aerosols using temperature-programmed thermal desorption particle beam mass spectrometry. *Anal. Chem.* **1999**, *71*, 3428−3435.

(16) (a) You, C.-Y.; Fan, X.; Zheng, A.-L.; Wei, X.-Y.; Zhao, Y.-P.; Cao, J.-P.; Zhao, W.; Zhou, C.-C.; Zhu, J.-L.; Chen, L.; et al. Molecular characteristics of a Chinese coal analyzed using mass spectrometry with various ionization modes. *Fuel* **2015**, *155*, 122−127. (b) Wang, S.-Z.; Fan, X.; Zheng, A.-L.; Wang, Y.-G.; Dou, Y.-Q.; Wei, X.-Y.; Zhao, Y.-P.; Wang, R.-Y.; Zong, Z.-M.; Zhao, W. Evaluation of atmospheric solids analysis probe mass spectrometry for the analysis of coal-related model compounds. *Fuel* **2014**, *117*, 556−563.

(17) Zhang, W.; Andersson, J. T.; Räder, H. J.; Müllen, K. Molecular characterization of large polycyclic aromatic hydrocarbons in solid petroleum pitch and coal tar pitch by high resolution MALDI ToF MS and insights from ion mobility separation. *Carbon* **2015**, *95*, 672−680.

(18) Dow, A. R.; Wittrig, A. M.; Kenttämaa, H. I. Laser-induced acoustic desorption mass spectrometry. *Eur. J. Mass Spectrom.* **2012**, *18*, 77−92.

(19) Ma, X.; Zhang, Y.; Lei, H.-R.; Kenttämaa, H. I. Laser-induced acoustic desorption. *MRS Bull.* **2019**, *44*, 372−381.

(20) Crawford, K. E.; Campbell, J. L.; Fiddler, M. N.; Duan, P.; Qian, K.; Gorbaty, M. L.; Kenttämaa, H. I. Laser-induced acoustic desorption/Fourier transform ion cyclotron resonance mass spectrometry for petroleum distillate analysis. *Anal. Chem.* **2005**, *77*, 7916−7923.

(21) Dreisewerd, K. The desorption process in MALDI. *Chem. Rev.* **2003**, *103*, 395−426.

(22) King, R.; Bonfiglio, R.; Fernandez-Metzler, C.; Miller-Stein, C.; Olah, T. Mechanistic investigation of ionization suppression in electrospray ionization. *J. Am. Soc. Mass Spectrom.* **2000**, *11*, 942−950.

(23) (a) Benham, K.; Hodyss, R.; Fernández, F. M.; Orlando, T. M. Laser-Induced Acoustic Desorption Atmospheric Pressure Photoionization via VUV-Generating Microplasmas. *J. Am. Soc. Mass Spectrom.* **2016**, *27*, 1805−1812. (b) Jarrell, T. M.; Owen, B. C.; Riedeman, J. S.; Prentice, B. M.; Pulliam, C. J.; Max, J.; Kenttämaa, H.

I. Laser-Induced Acoustic Desorption/Electron Ionization of Amino Acids and Small Peptides. *J. Am. Soc. Mass Spectrom.* **2017**, *28*, 1091−1098. (c) Campbell, J. L.; Crawford, K. E.; Kenttämaa, H. I. Analysis of saturated hydrocarbons by using chemical ionization combined with laser-induced acoustic desorption/Fourier transform ion cyclotron resonance mass spectrometry. *Anal. Chem.* **2004**, *76*, 959−963.

(24) Jia, L.; Weng, J.; Zhou, Z.; Qi, F.; Guo, W.; Zhao, L.; Chen, J. Note: Laser-induced acoustic desorption/synchrotron vacuum ultraviolet photoionization mass spectrometry for analysis of fragile compounds and heavy oils. *Rev. Sci. Instrum.* **2012**, *83*, 026105.

(25) Chen, J.; Jia, L.; Zhao, L.; Lu, X.; Guo, W.; Weng, J.; Qi, F. Analysis of Petroleum Aromatics by Laser-Induced Acoustic Desorption/Tunable Synchrotron Vacuum Ultraviolet Photoionization Mass Spectrometry. *Energy Fuels* **2013**, *27*, 2010−2017.

(26) (a) Weng, J.; Jia, L.; Wang, Y.; Sun, S.; Tang, X.; Zhou, Z.; Kohse-Höinghaus, K.; Qi, F. Pyrolysis study of poplar biomass by tunable synchrotron vacuum ultraviolet photoionization mass spectrometry. *Proc. Combust. Inst.* **2013**, *34*, 2347−2354. (b) Qi, F.; Yang, R.; Yang, B.; Huang, C.; Wei, L.; Wang, J.; Sheng, L.; Zhang, Y. Isomeric identification of polycyclic aromatic hydrocarbons formed in combustion with tunable vacuum ultraviolet photoionization. *Rev. Sci. Instrum.* **2006**, *77*, 084101.

(27) Petroleum and Natural Gas Industry Standard of the People's Republic of China SY/T 5119-2008.

(28) Xiong, Y.; Jin, L.; Li, Y.; Zhou, Y.; Hu, H. Structural Features and Pyrolysis Behaviors of Extracts from Microwave-Assisted Extraction of a Low-Rank Coal with Different Solvents. *Energy Fuels* **2019**, *33*, 106−114.

(29) Yu, J. X.; Chen, Y. W.; Zhang, J. L.; Chen, S. J.; Wang, Q. L.; Qin, Z. B.; Tang, Z. C. Development of a miniature time-of-flight mass spectrometer coupled with an improved substrateenhanced laser-induced acoustic desorption source (SE-LIAD/TOF-MS). *Analyst* **2021**, *146* (13), 4365−4373.

(30) He, J.; Huang, R.-J.; Li, G.; Tang, Z.-C.; Lin, S.-C. Development of a Miniature High Resolution Electron Impact Ion Source Time-of-Flight Mass Spectrometer. *Chin. J. Anal. Chem.* **2013**, *40*, 1616−1621.

(31) Yu, J.; Chen, Y.; Zhang, J.; Chen, S.; Wang, Q.; Qin, Z.; Tang, Z. Development of a miniature time-of-flight mass spectrometer coupled with an improved substrate-enhanced laser-induced acoustic desorption source (SE-LIAD/TOF-MS). *Analyst* **2021**, *146*, 4365−4373.

(32) (a) Schwarz, F. P.; Smith, D.; Lias, S. G.; Ausloos, P. The Fluorescence and Photofragmentation of Liquid Saturated-Hydrocarbons at Energies above the Photo-Ionization Threshold. *J. Chem. Phys.* **1981**, *75*, 3800−3808. (b) Nir, E.; Hunziker, H. E.; de Vries, M. S. Fragment-free mass spectrometric analysis with jet cooling VUV photoionisation. *Anal. Chem.* **1999**, *71*, 1674−1678.

(33) (a) Eschner, M. S.; Zimmermann, R. Determination of Photoionization Cross-Sections of Different Organic Molecules Using Gas Chromatography Coupled to Single-Photon Ionization (SPI) Time-of-Flight Mass Spectrometry (TOF-MS) with an Electron-Beam-Pumped Rare Gas Excimer Light Source (EBEL): Influence of Molecular Structure and Analytical Implications. *Appl. Spectrosc.* **2011**, *65*, 806−816. (b) Jin, H.; Yang, J.; Farooq, A. Determination of absolute photoionization cross-sections of some aromatic hydrocarbons. *Rapid Commun. Mass Spectrom.* **2020**, *34*, 11.

(34) (a) Stanger, R.; Tran, Q. A.; Attalla, T.; Smith, N.; Lucas, J.; Wall, T. The pyrolysis behaviour of solvent extracted metaplast material from heated coal using LDI-TOF mass spectroscopy measurements. *J. Anal. Appl. Pyrolysis* **2016**, *120*, 258−268. (b) Marzec, A. Towards an understanding of the coal structure: a review. *Fuel Process. Technol.* **2002**, *77*−*78*, 25−32.

(35) Li, W.; Ye, C.; Feng, J.; Xie, K. Influence of column chromatography and Soxhlet extraction on the composition of coal pyridine soluble. *Chin. J. Anal. Chem.* **2006**, *34*, 905−910.

(36) Katoh, T.; Yokoyama, S.; Sanada, Y. Analysis of a coal-derived liquid using high-pressure liquid-chromatography and synchronous fluorescence spectrometry. *Fuel* **1980**, *59*, 845−850.

(37) Wang, Z.; Wei, C.; Shui, H.; Ren, S.; Pan, C.; Wang, Z.; Li, H.; Lei, Z. Synchronous fluorimetric characterization of heavy intermediates of coal direct liquefaction. *Fuel* **2012**, *98*, 67−72.

(38) Li, Y.; Michels, R.; Mansuy, L.; Fleck, S.; Faure, P. Comparison of pressurized liquid extraction with classical solvent extraction and microwave-assisted extraction-application to the investigation of the artificial maturation of Mahakam coal. *Fuel* **2002**, *81*, 747−755.

(39) Bissada, K. K.; Tan, J.; Szymczyk, E.; Darnell, M.; Mei, M. Group-type characterization of crude oil and bitumen. Part I: Enhanced separation and quantification of saturates, aromatics, resins and asphaltenes (SARA). *Org. Geochem.* **2016**, *95*, 21−28.

(40) Dutta, T. K.; Harayama, S. Time-of-flight mass spectrometric analysis of high-molecular-weight alkanes in crude oil by silver nitrate chemical ionization after laser desorption. *Anal. Chem.* **2001**, *73*, 864−869.

(41) Heberle, H.; Meirelles, G. V.; da Silva, F. R.; Telles, G. P.; Minghim, R. InteractiVenn: a web-based tool for the analysis of sets through Venn diagrams. *BMC Bioinf.* **2015**, *16*, 7.

(42) Xiong, Y.; Jin, L.; Li, Y.; Zhu, J.; Hu, H. Hydrogen peroxide oxidation degradation of a low-rank Naomaohu coal. *Fuel Process. Technol.* **2020**, *207*, 106484.

https://doi.org/10.1021/acsomega.1c06619
ACS Omega 2022, 7, 6935−6943